Cytokine-inducible enhancer with promoter activity in both the rat and human manganese-superoxide dismutase genes

Richard J. ROGERS†‡, Sarah E. CHESROWN‡§, Shiuhyang KUO*, Joan M. MONNIER* and Harry S. NICK*†§[1]

*Department of Neuroscience, Box 100244 HSC, University of Florida College of Medicine, Gainesville, FL 32610, U.S.A., †Department of Biochemistry and Molecular Biology, University of Florida College of Medicine, Gainesville, FL, U.S.A., ‡Department of Anesthesiology, University of Florida College of Medicine, Gainesville, FL, U.S.A., and §Department of Pediatrics, University of Florida College of Medicine, Gainesville, FL, U.S.A.

Diverse pro-inflammatory mediators regulate transcription of the gene (*MnSOD*) encoding the mitochondrial anti-oxidant protein manganese-superoxide dismutase. Understanding the regulation of this gene is crucial to comprehending its role in cytoprotection. In transfected lung epithelial cells, a human-growth-hormone reporter gene system was utilized to identify a potential enhancer in the MnSOD genomic fragment previously shown to contain multiple DNase-I-hypersensitive sites. Northern analysis demonstrated a 10–20-fold increase in response to pro-inflammatory mediators. Inclusion of the MnSOD genomic fragment in reporter constructs was necessary to mimic these stimulus-dependent endogenous levels. The inducible enhancer element was localized to a 260 bp fragment in intron 2, coinciding with a previously defined DNase-I-hypersensitive site. This element functions in an orientation- and position-independent manner as well as with the heterologous thymidine kinase promoter. In addition, we have demonstrated that a homologous sequence within the human *MnSOD* gene exhibits identical enhancer activity. A novel characteristic of the rat and human enhancer elements involves the ability to promote cytokine-inducible transcription in the absence of a classical promoter.

Key words: anti-oxidant, cytokines, cytoprotection, gene regulation.

INTRODUCTION

The superoxide dismutases (SODs) are the first line of cellular defence against the damaging effects of superoxide anion radicals [1]. Manganese-superoxide dismutase (MnSOD) is a highly regulated SOD [2,3], being localized to mitochondria [4,5] and conferring potent cytoprotective potential [6–13]. Multiple studies have shown that increased cellular levels of MnSOD are cytoprotective during cellular oxidative stress [6] or inflammatory challenges: tumour-necrosis-factor-α (TNF-α)-mediated apoptosis [7,8], interleukin-1 (IL-1) cytotoxicity [9], ionizing radiation [10,11] and neurotoxicity [12,13]. The role of MnSOD as a cytoprotective enzyme is most strikingly illustrated in three transgenic mouse models. The first involves targeted over-expression of *MnSOD* in the pulmonary epithelium of mice, resulting in a decreased level of inflammation, and increased survival as a consequence of a hyperoxic exposure [14]. The physiological importance of this gene is best exemplified through gene ablation where *MnSOD* knockout mice manifest severe dilated cardiac myopathy and die within 10 days of birth [15]. The third study shows that treatment of the *MnSOD* knockout mouse with a superoxide dismutase mimic, manganese 5,10,15,20-tetrakis-(4-benzoic acid)porphyrin, rescues these mice from the systemic toxicity, but allows development of a severe neurodegenerative disorder by 3 weeks of age [16].

Previous investigations from this and other laboratories have established that levels of steady-state MnSOD mRNA and protein increase following exposure to bacterial lipopolysaccharide, tumour necrosis factor and interleukin-1 [2,7,9,16]. Stimulus-dependent increases in mRNA levels are inhibited by actinomycin D [17], suggesting increased *de novo* transcription, which has been confirmed by subsequent nuclear run-on studies [17a]. Results from DNase-I-hypersensitivity studies analysing the chromatin structure of *MnSOD* have identified multiple regions of increased nuclease accessibility located throughout the gene as well as a stimulus-dependent alteration in chromatin structure in the 5′ flanking region [18]. Furthermore, dimethyl sulphate *in vivo* footprinting studies have identified the binding sites for ten basal protein factors which interact with the promoter as well as stimulus-dependent alterations in guanine-residue-reactivity near the hypersensitive site found only in stimulus-treated cells [18]. To complement the preceding studies on chromatin structure and *in vivo* footprinting, functional studies of the promoter analysed deletions of the 5′ flanking region. The promoter deletion data suggest that basal promoter activity requires only 500 bp of the 5′ flanking region. Together these data suggest that multiple protein–DNA interactions occur during transcription under basal conditions and that treatment with inflammatory mediators causes an alteration in chromatin structure in the promoter region of the gene.

Not all *cis*-acting regulatory elements are located in 5′ flanking regions. For example, regulatory sequences have been identified within introns or in distant 3′ flanking sequences of the human and mouse Igκ gene [19,20], platelet-derived-growth-factor gene [21], alcohol dehydrogenase-1-S gene [22] and collagen genes [23]. To identify regions of *MnSOD* that regulate basal and stimulated expression, our present study utilized deletion analysis of rat *MnSOD* [24] coupled with transient transfection studies in

Abbreviations used: (Mn)SOD, (manganese-)superoxide dismutase; TNF-α, tumour necrosis factor-α; IL-1, interleukin-1; LPS, lipopolysaccharide; hGH, human growth hormone; NF-κB, nuclear factor κB; C/EBP, CAAT-enhancer binding protein; EMSA, electrophoretic-mobility-shift assay; TK, thymidine kinase; GKLF, **g**ut-enriched **K**rüppel-**l**ike **f**actor.

[1] To whom correspondence should be sent (e-mail hnick@ufbi.ufl.edu).

a rat lung epithelial cell line. Measuring mRNA expression levels of the human-growth-hormone (hGH) reporter gene, we have localized a complex enhancer element within intron 2 of the rat and a homologous region in intron 2 of the human *MnSOD*. Most interestingly, this regulatory element possesses the ability to promote cytokine-inducible transcription independent of a promoter sequence.

EXPERIMENTAL

Cell culture and transfection

L2 cells, a rat pulmonary epithelial-like cell line (A.T.C.C. CCL 149), were grown in Ham's modified F12K medium (GIBCO) with 10% fetal bovine serum (Flow Laboratories), ABAM [penicillin G (100 units/ml)/streptomycin (0.1 mg/ml)/amphotericin B (0.25 μg/ml)] (Sigma) and 4 mM glutamine at 37 °C in room air/5% CO_2. All transfections were performed using a batch transfection method in at least three individual experiments with each plasmid construct. This transfection method allowed comparison of control and stimulus-inducible transcription for the individual plasmid constructs. Transfection efficiency between individual plasmid constructs was examined using a β-galactosidase vector (pcDNA3.1/HisB/*lac*Z, Invitrogen). Cells were grown as monolayers on 150-mm diameter tissue-culture plates until 70–90% confluent. The cells were transfected with 10 μg of each expression vector using the DEAE-dextran method [25]. After 24 h, cells from each 150-mm-diameter batch-transfected plate were trypsin-treated, pooled, and plated on to four separate 100-mm-diameter tissue-culture plates. Inflammatory mediators were added to the medium of each plate 24 h later with final concentrations of 0.5 μg/ml *Escherichia coli* lipopolysaccharide (LPS; *E. coli* serotype 055:B5, Sigma), 10 ng/ml TNF-α (kindly provided by the Genentech Corp., San Francisco, CA, U.S.A.), or 2 ng/ml IL-1β (kindly provided by the National Cancer Institute). After 24 h, total RNA was isolated from the cell monolayers for Northern analysis.

RNA isolation and Northern analysis

Inducible gene expression in transfected cells was analysed by directly measuring hGH mRNA levels. Total RNA was isolated by the guanidinium thiocyanate/phenol/chloroform extraction method described by Chomczynski and Sacchi [26], with modifications as previously described [9]. A 20 μg portion of RNA was size-fractionated on a 1%-denaturing-agarose gel, transferred to a nylon membrane and UV-cross-linked. Membranes were hybridized with ^{32}P-labelled human hGH, and rat cathepsin B (loading control) cDNA probes made by random primer extension. Some membranes were also hybridized with a ^{32}P-labelled rat MnSOD probe to assess simultaneous induction of the endogenous MnSOD.

Construction of expression vectors

A 4.5 kb *Eco*RI/*Eag*I fragment of 5′ non-coding sequence was isolated from the 17 kb *MnSOD* genomic clone and the 5′ overhanging ends filled in using the large fragment of *E. coli* DNA polymerase I (Klenow fragment). The resulting blunt-end *Eco*/*Eag* fragment was cloned into the *Hin*cII polylinker site in a promoter-less, pUC 12-based hGH expression vector, pΦGH, [27], creating a 9.3 kb plasmid referred to as Eco/E GH. The unique restriction enzyme sites *Hin*dIII, *Sfi*I, *Sac*II and *Nae*I were utilized to create deletions of the *MnSOD* Eco/E sequence, creating the vectors Hind/E, Sfi/E, Sac/E, and Nae/E as previously described [18]. To test for non-specific effects of the inflammatory mediators on hGH expression, we used an hGH expression vector that contained the herpes simplex thymidine kinase minimal promoter pTKGH [27].

To identify possible regulatory elements in the remainder of *MnSOD* that might interact with the 5′ promoter, we cloned an internal 6.1 KB *Hin*dIII fragment (+1180 to +7312) from the rat genomic clone into the *Hin*dIII site of the Hind/E GH vector, creating a 13.45 kb vector (Figure 1, top panel). The same *Hin*dIII fragment was cloned into Hind/E GH in the opposite orientation. To begin to localize observed enhancer effects, we removed the *Hin*dIII/*Hpa*I fragment (+1180 to +5046) and the *Hpa*I/*Hin*dIII fragment (+5046 to +7312) from the *Hin*dIII fragment in both orientations, creating enhancer deletions of 3.8 kb or 2.3 kb in the Hind/E GH construct (Figure 1, top panel). To clarify the position of the enhancer within the 3.8 kb fragment, serial 3′ and 5′ deletions of the area were performed by creating PCR products (Figures 2 and 3, top panels) which were subsequently cloned into the Hind/E GH vector at the *Hin*dIII site or *Nde*I site. Oligonucleotides flanking the regions of interest were designed containing either *Hin*dIII or *Nde*I sites for convenient ligation into the restriction sites. To test whether the enhancer activity was specific to the *MnSOD* promoter, we used the plasmid pTKGH, which contains a heterologous TATA-containing, non-GC-rich viral promoter. The 6.1 kb *Hin*dIII MnSOD genomic fragment (+1180 to +7312) was cloned into the *Hin*dIII site (Figure 4, left panel) in the TKGH polylinker in both orientations. To evaluate the interaction of the promoter with the enhancer fragment, the 919 bp (see Figures 2A and 5A) fragment of *MnSOD* containing the entire enhancer region was ligated into the *Nde*I site of the promoter deletion constructs previously described (Figure 5, top panel) [18].

Comparison of the rat enhancer sequence with the analogous region in human *MnSOD* revealed a high degree of similarity in intron 2. PCR amplification of a 466 bp fragment (+2410 to +2875, human MnSOD, accession no. S77127) from human genomic DNA using primers (5′ CGTTAGTGGTTTGCACA-AGGAAGATAATCG 3′ and 5′ GGCTCTGATTCCACAA-GTAAAGGACTG 3′) created a fragment which was inserted into *Nde*I site of the TKGH vector in both orientations. The same 466 bp human enhancer fragment and the 260, 553 or 746 bp rat enhancer fragment were ligated into the *Hin*dIII site of the pΦGH vector (Figure 6, left panel).

Electrophoretic-mobility-shift assays (EMSAs)

EMSAs were performed as previously described [28] with 8 μg nuclear extract prepared from control and LPS, TNF-α, or IL-1β-treated L2 cells by high salt extraction [29]. Binding reactions were carried out at room temperature in 10 mM Hepes (pH 7.9)/100 mM KCl/1mM dithiothreitol/0.5 mM $MgCl_2$/0.1 mM EDTA/8.5% (v/v) glycerol to yield a final volume of 20 μl. EMSA probes were made from cloned PCR products of the defined enhancer region between 4130 and 4491 and end-labelled by filling the recessed 3′ termini of *Eco*RI-digested fragments with [^{32}P]dATP using the large fragment of *E. coli* DNA polymerase I (Klenow fragment). Fragments used in EMSAs were 143 bp (+4348 to +4491), 143 bp (+4231 to +4374), 100 bp (+4231 to +4331), 95 bp (+4331 to +4426), and 103 bp (+4426 to +4529). Numbers in parentheses refer to the sequence in rat *MnSOD* (accession no. X56600).

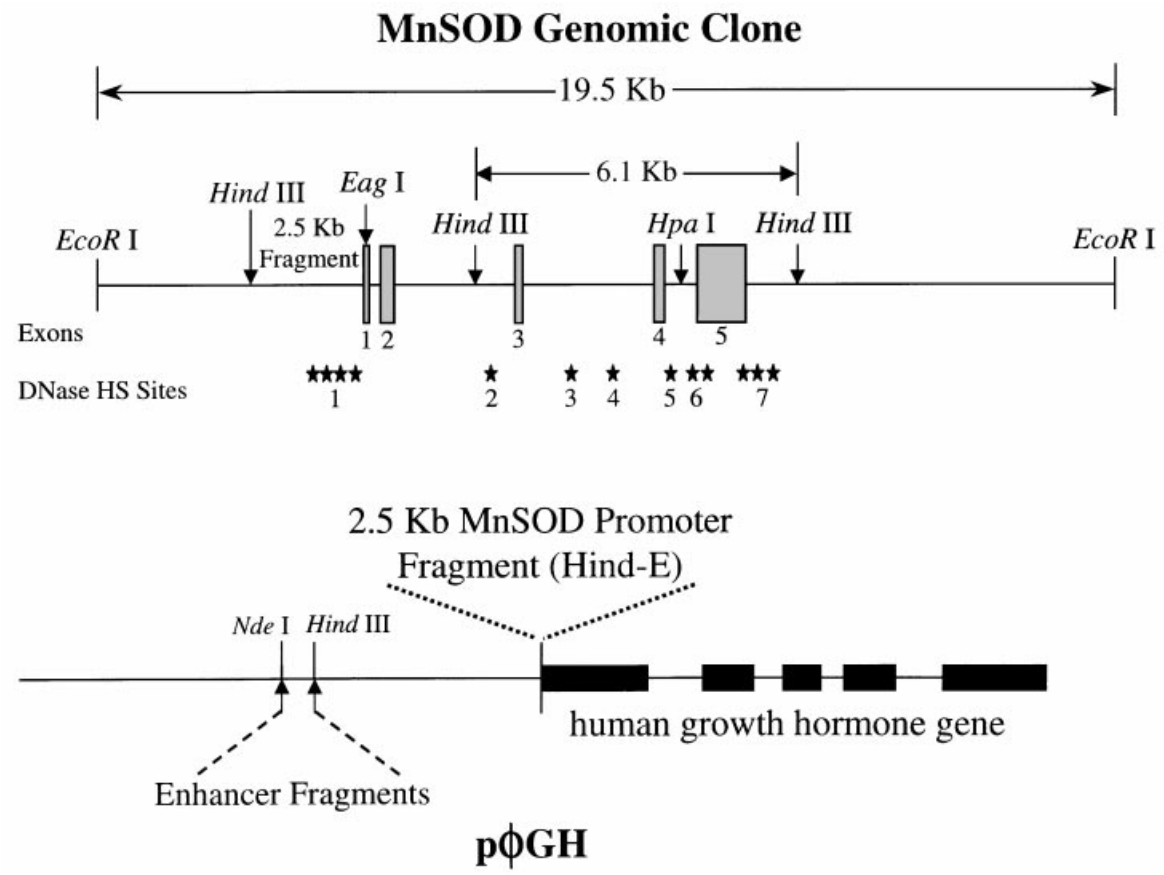

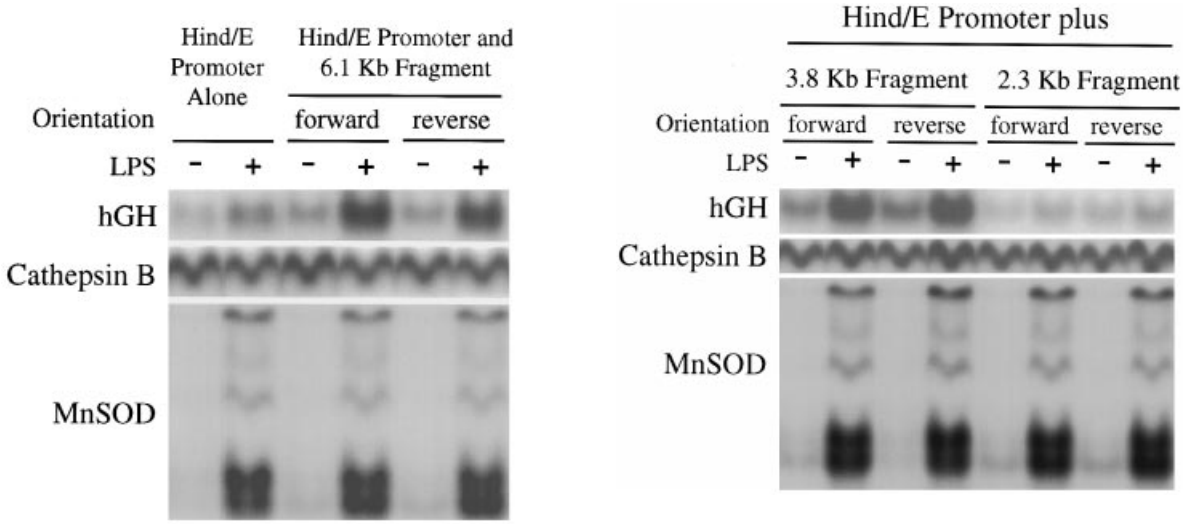

Figure 1 Identification of an enhancer within the MnSOD gene

Top panel: schematic representations and restriction maps of the *MnSOD* genomic clone and the expression vectors constructed to assess potential enhancer activity. The restriction enzyme sites are indicated above the sequence (e.g., *Hin*dIII). The expression vectors contain the 6.1 kb *Hin*dIII fragment from positions +1197 to +7238 of *MnSOD*, with DNase-I-hypersensitive sites 2–7 (*; [18]) in either the 5′-to-3′ or the 3′-to-5′ orientation. In addition, each expression vector contains the *MnSOD* 5′ promoter sequence from the *Hin*dIII site to the *Eag*I site (Hind-E). The *Hin*dIII fragment, from positions +1107 to +7238 of *MnSOD*, has been cut at position +4938 by *Hpa*I digestion creating the 3.8 kb and 2.3 kb fragments. The *Hin*dIII (+1107) to *Hpa*I (+4938) fragment contains hypersensitive sites 2, 3 and 4 (*; [18]). The *Hpa*I (+4938) to *Hin*dIII (+7238) fragment contains hypersensitive sites 5, 6 and 7. These two fragments were tested in transient transfections as was the 6.1 kb *Hin*dIII fragment. The restriction sites (*Hin*dIII and *Nde*I) into which the enhancer deletions were ligated are denoted on hGH vector, which also contains *MnSOD* promoter (Hind-E). Bottom left panel: hGH mRNA levels after transfection in rat lung epithelial cells with vectors containing the internal *Hin*dIII fragment of *MnSOD* coupled to the promoter versus *MnSOD* promoter alone. Northern analysis was done using radiolabelled probes synthesized from hGH, MnSOD and cathepsin B cDNAs as described in the Experimental section. Bottom right panel: hGH mRNA expression in rat lung epithelial cells transfected with vectors containing either the 3.8 kb or the 2.3 kb fragments which are deletions of the internal *Hin*dIII fragment of *MnSOD*.

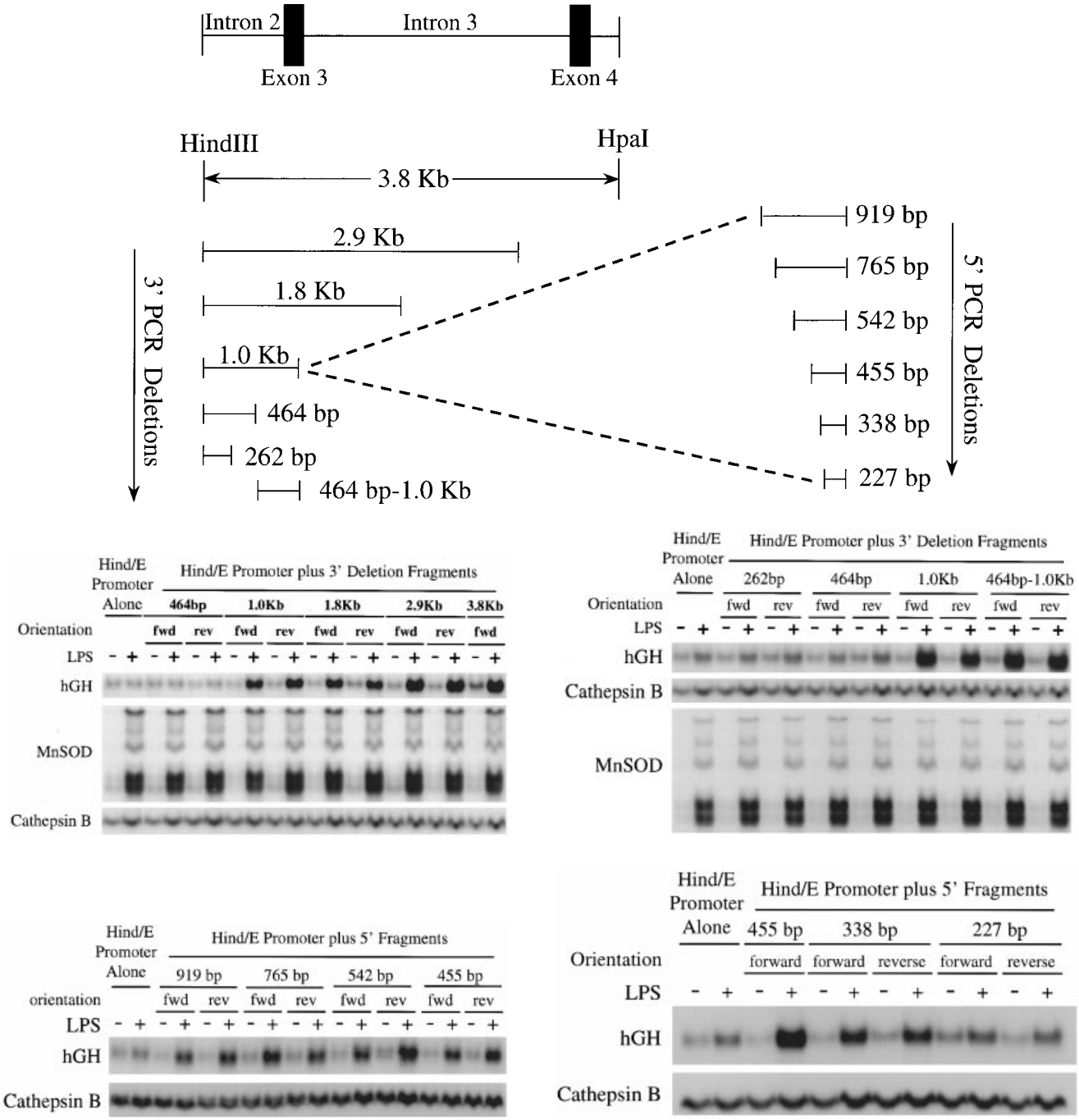

Figure 2 Deletion analysis of the *MnSOD* enhancer

Top panel, deletions of the 3.8 kb enhancer fragment. Serial deletions from both the 5′ and 3′ ends of the 3.8 kb fragment were created by PCR amplification and ligated into either the *Hin*dIII site or the *Nde*I site of the Hind/E GH vector (see Figure 1, top panel). Middle left and right panels: Northern analysis of transient transfections of the 3′ PCR deletions of the 3.8 kb enhancer fragment localized the inducible activity to the 464 bp/1.0 kb fragment by Northern analysis. Bottom left and right panels: transient transfections and Northern analysis of the 5′ PCR deletions of the 3.8 kb enhancer fragment localized the inducible activity to an area between the 455 bp and the 227 bp fragments in the 3′ end of the 1.0 kb PCR fragment.

RESULTS

An inducible *cis*-acting enhancer element exists within *MnSOD*

Previous results of steady-state MnSOD mRNA levels in rat pulmonary epithelial and endothelial cells demonstrated dramatic induction with inflammatory mediators [2]. In addition, nuclear run-on experiments showed that stimulus-dependent *MnSOD* expression is at least in part a consequence of *de novo* transcription [18]. *MnSOD* promoter deletion analysis demonstrated levels of stimulus-dependent *MnSOD* expression that were far lower than that seen with the endogenous steady-state mRNA. The vector constructs used in the analysis contained only 5′ flanking sequence, incorporating only one of the seven DNase-I-hypersensitive sites within *MnSOD* [18]. To determine whether the

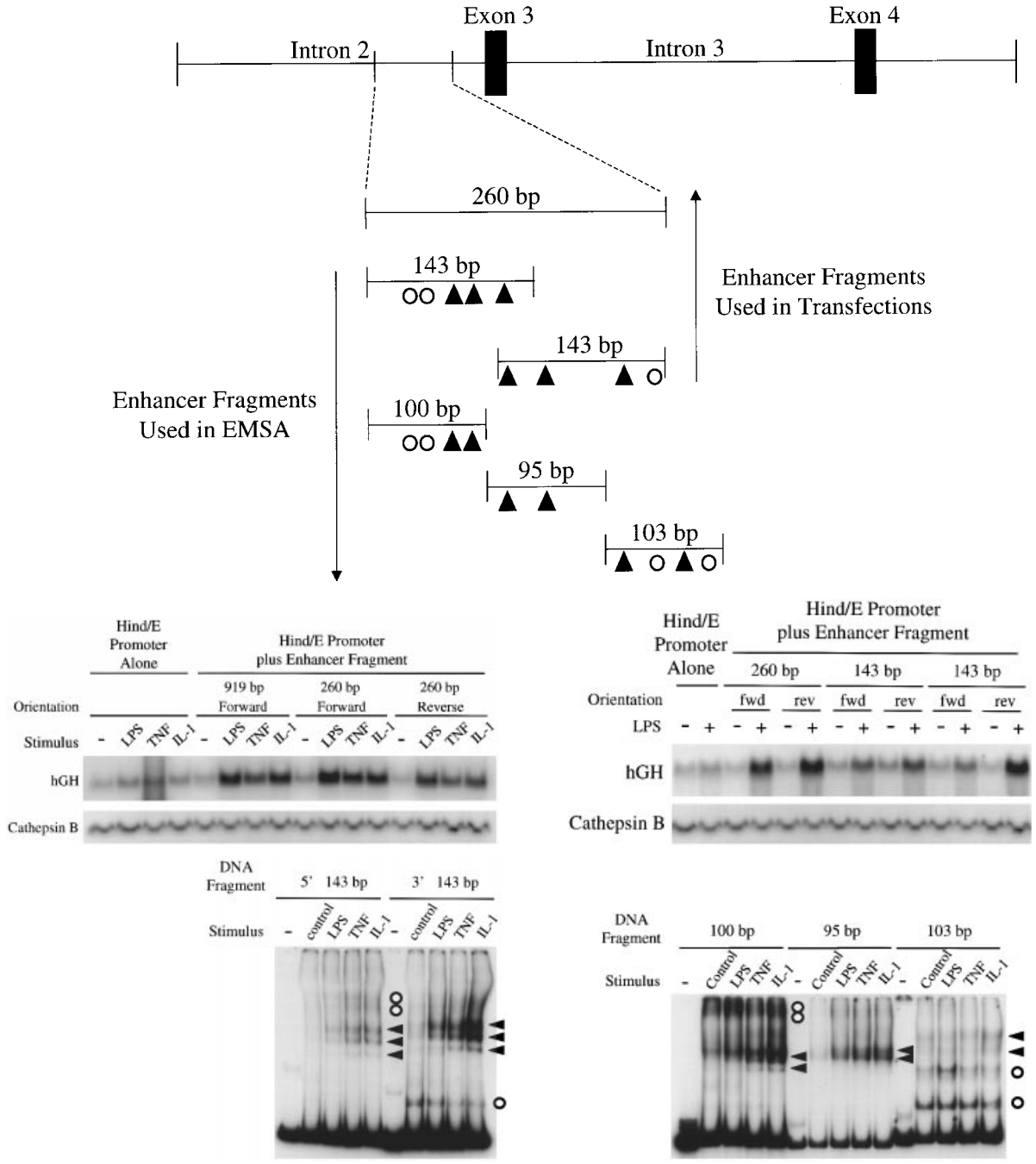

Figure 3 Evaluation of the 260 bp enhancer region

Top panel: schematic of the enhancer region in intron 2. A 260 bp PCR fragment of the enhancer region totally contained within intron 2 and two overlapping 143 bp PCR fragments encompassing the 260 bp region were created and ligated into the *Nde*I site of the Hind/E GH vector (see Figure 1, top panel) for transient transfection in rat epithelial cells and Northern analysis. In addition to the 143 bp fragments, three other fragments (100, 95 and 103 bp) were created by PCR amplification for EMSA. Putative constitutive and inducible protein-binding sites are illustrated by open circles and filled triangles respectively. Middle left panel: Northern analysis of transient transfections of the 919 bp (see Figure 2, top panel) or the 260 bp fragment (both orientations) in the Hind/E GH vectors in control and LPS, TNF-α, and IL-1β-stimulated rat pulmonary epithelial cells. Middle right panel: Northern analysis of transient transfections of the 260 bp fragment and 143 bp fragments in the Hind/E GH vectors in control and LPS-stimulated rat pulmonary epithelial cells. Bottom left and right panels: EMSA of the two 143 bp, as well as of the 100, 95 and 103 bp fragments using nuclear extracts from untreated cells and cells treated with LPS, TNF-α, and IL-1β. Open circles refer to putative constitutive protein binding and filled triangles refer to putative inducible protein binding.

remaining DNase-I-hypersensitive sites within *MnSOD* contained regulatory function, we created hGH expression vectors that combine both the *MnSOD* promoter (a 2.5 kb *Hin*dIII-to-*Eag*I fragment) and a 6.1 kb *Hin*dIII fragment, containing the remaining DNase-I-hypersensitive sites (Figure 1A). Expression of *hGH* in cells transfected with these vectors was compared in

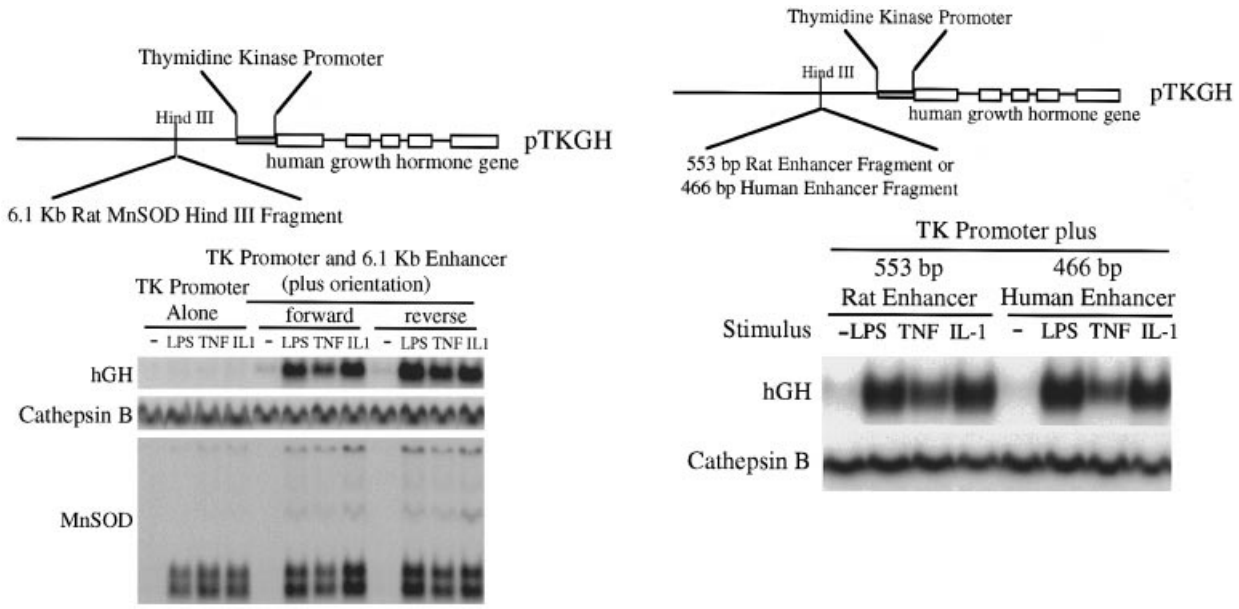

Figure 4 Functional analysis of the *MnSOD* enhancer with the TK promoter

Left panel: interaction of the 6.1 kb *MnSOD* fragment with the heterologous herpes-simplex TK promoter in the pTKGH expression vector. Expression vectors, pTKGH alone and pTKGH containing the 6.1 kb enhancer (both orientations), were constructed and a comparison of hGH mRNA levels in transiently transfected rat lung epithelial cells treated with LPS, TNF-α or IL-1β was made. Northern analysis was done using radiolabelled probes synthesized from hGH, MnSOD and cathepsin B cDNAs. Right panel: comparison of the rat and human enhancer regions in the pTKGH vector. A 553 bp region encompassing the rat enhancer as well as the analogous region of the human *MnSOD* (466 bp fragment) were amplified by PCR and cloned into the *Hin*dIII site of the pTKGH vector. Northern analysis of transient transfections in rat pulmonary epithelial cells shown here is described in the Experimental section.

the same experiments with expression of *hGH* in cells transfected with the vector construct Hind/E GH, containing only the 5′ promoter fragment.

Of note, the data displayed in Figure 1, bottom left panel, and all subsequent Figures, use Northern analysis to directly assess transcription rates from the transfected reporter constructs. This is distinct from studies which assay reporter protein levels or enzymic activity that must take into consideration potential effects of stimuli on translation and post-translational events.

As shown in Figure 1, bottom left panel, LPS treatment caused a dramatic enhancement of steady-state mRNA expression as a result of adding the internal MnSOD genomic fragment, in a manner independent of fragment orientation. The same result was obtained when transfected cells were stimulated with TNF-α or IL-1β (results not shown). Furthermore, cleavage of the 6.1 kb *Hin*dIII fragment by making use of the unique *Hpa*I site demonstrated that the *cis*-acting element responsible for the inducible activity was localized to the 5′ 3.8 kb portion of the original *Hin*dIII fragment (Figure 1, bottom right panel). Again, orientation did not influence the inducible activity in response to inflammatory mediators, thus indicating that the element could partially satisfy the definition of an enhancer.

The *MnSOD* inducible enhancer element is located within intron 2

To localize the inducible *cis*-acting element within the 3.8 kb region, a set of serial deletion fragments spanning this region were amplified by PCR using complementary oligonucleotides and inserted into the *MnSOD* promoter vector, Hind-E GH. Deletions of the fragment from the 5′ end and from the 3′ end (Figure 2, top panel) were generated in this manner. The inducible enhancer activity was evaluated by transient transfections into L2 cells using Northern analysis. On the basis of the 3′ deletions of the 3.8 kb *Hin*dIII–*Hpa* I fragment, the enhancer activity was localized to a region of approx. 450 bp in the 5′ end of this 3.8 kb fragment (Figure 2, middle left and right panels). This position coincides extremely well with DNase-hypersensitive site 2 [18] located near the intron 2/exon 3 boundary.

In an effort to localize the enhancer more precisely, 5′ deletions were also constructed as shown in Figure 2 (bottom left and right panels). Multiple 3′ and 5′ deletions containing the enhancer fragment demonstrate inducible activity comparable with the steady-state mRNA levels of the endogenous gene. Interestingly, the 338 and 227 bp deletions show diminished enhancer activity relative to the 455 bp fragment, as shown in Figure 2, bottom right panel, thus delineating the enhancer activity regulated by LPS, TNF-α and IL-1β to within a 200–300 bp region near the 3′ end of intron 2.

The enhancer is likely composed of a complex set of interacting elements

To further localize the enhancer within the 3′ end of intron 2, additional deletion constructs were created (Figure 3, top panel). PCR amplification was used to generate a 260 bp fragment spanning the region between the two 5′ deletions shown in Figure 2, top panel (455 and 227 bp), as well as two 143 bp fragments which overlap each other within the 260 bp fragment (Figure 3, top panel). The ability of these fragments to cause inducible expression was evaluated by transient transfection and Northern analysis. The 260 bp fragment reproduced the enhancer activity seen with the larger 919 bp fragment (Figure 3, middle left

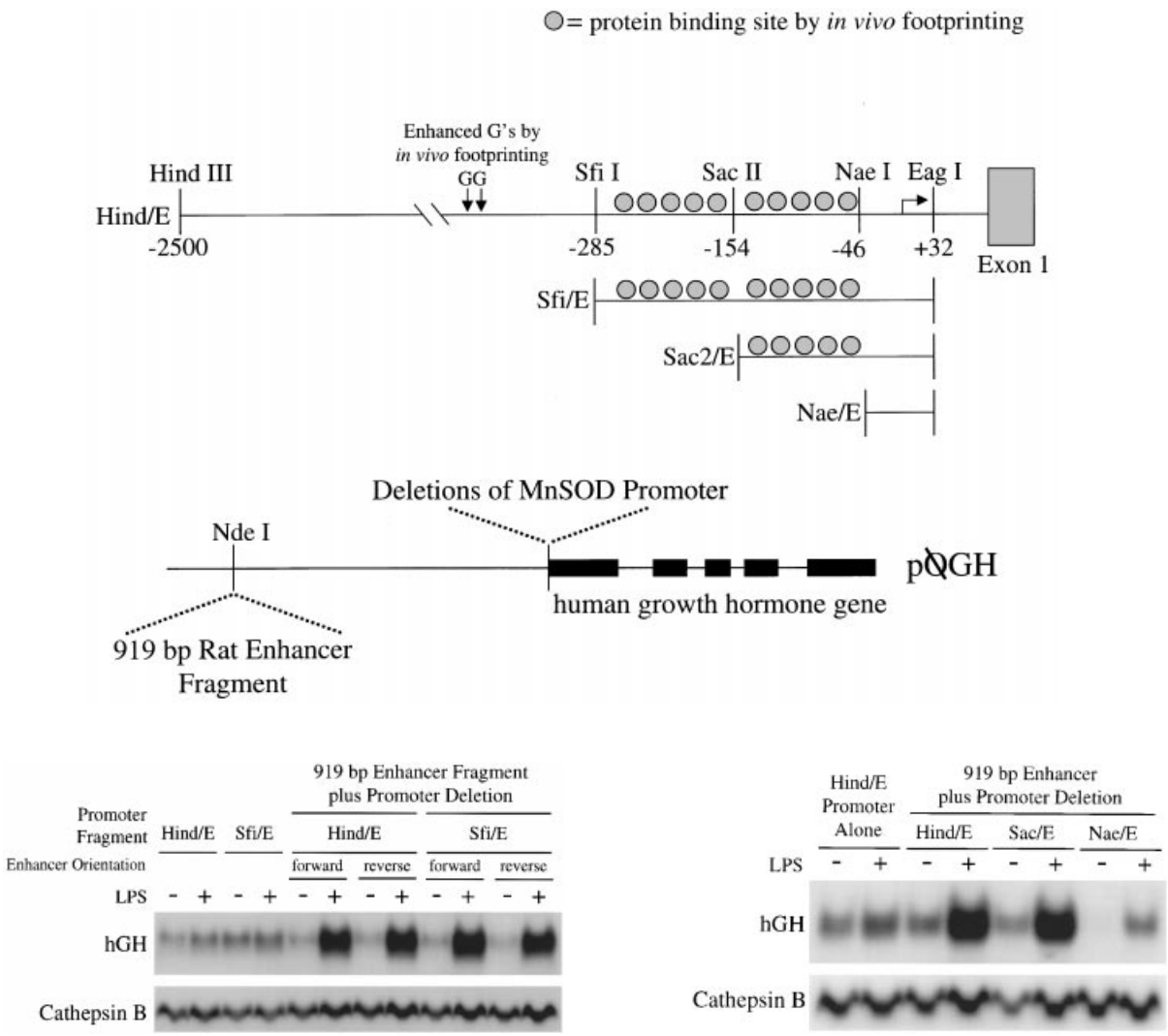

Figure 5 Functional interaction of the enhancer with deletions of the *MnSOD* promoter

Top panel: *MnSOD* promoter deletions summarizing the protein binding sites found by *in vivo* footprinting [18]. The 919 bp fragment encompassing the entire enhancer was ligated into the *Nde*I site of the hGH vector with the respective *MnSOD* promoter deletions. Bottom left panel: Northern analysis following transient transfections of promoter deletion constructs (Hind/E and Sfi/E containing the 919 bp enhancer fragment) into rat pulmonary epithelial cells. Bottom right panel: promoter deletions Hind/E, Sac/E and Nae/E containing the 919 bp enhancer fragment were transfected into rat pulmonary epithelial cells followed by Northern analysis.

panel). In addition, response to all the inflammatory mediators (LPS, TNF-α and IL-1β) was maintained. Interestingly, the two overlapping 143 bp fragments show reproducibly diminished enhancer activity as compared with the 260 bp fragment (Figure 3, middle right panel). These results are consistent with the previous deletion analyses in Figure 2, bottom right panel, which showed partial enhancer activity in the 338 bp fragment compared with the 455 bp fragment and loss of activity with the 227 bp fragment. Together the results summarized in Figures 2 (bottom right panel) and 3 (middle right panel) demonstrate that the 260 bp fragment likely delineates the minimum functional boundaries of the enhancer. In addition, the complexity and interactive nature of this important regulatory sequence are displayed by the retention of enhancer activity in the 143 bp fragments relative to the promoter alone.

To further assess the complexity of the enhancer element, EMSAs were performed with nuclear extracts from control and treated (LPS, TNF-α, IL-1β) cells. Figure 3, bottom left panel, illustrates the different protein-binding patterns between treated and control nuclear extracts, as well as the different patterns of protein binding between the two functional DNA fragments of the enhancer element. Constitutive protein binding is observed in the 3′ 143 bp fragment, but several inducible binding proteins can be appreciated in both fragments. In an attempt to further localize the protein-binding sites, smaller fragments of the involved region were generated by PCR and evaluated by EMSA (Figure 3, bottom right panel). Once again, constitutive protein binding was observed in two of the fragments (100 bp and 103 bp). However, as with the 143 bp fragment, inducible protein binding was also observed in two of the smaller fragments (100 bp and 95 bp), most notably in the 95 bp fragment, with a dramatic difference in binding between control and stimulated nuclear extracts. Further localization of protein binding was attempted with 50 bp and 30 bp fragments from this region.

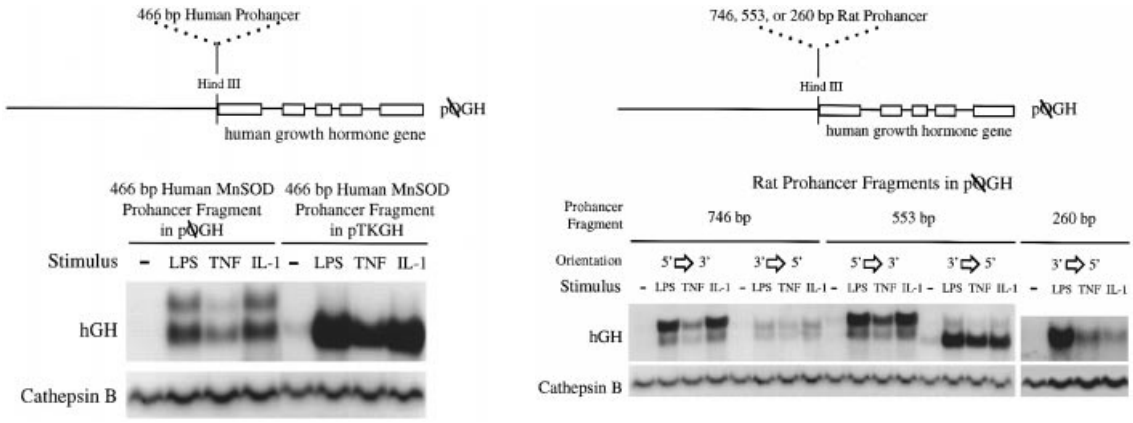

Figure 6 The *MnSOD* enhancer acting as a promoter

Left panel: schematic of the promoter-less human growth hormone vector (pΦGH) and the position of the human 466 bp enhancer fragment. Northern analysis of the 466 bp human enhancer in pΦGH and pTKGH constructs transiently transfected into control and treated (LPS, TNF-α, and IL-1β) rat pulmonary epithelial cells. Right panel: schematic of the promoter-less hGH vector (pΦGH) and the position of the 260, 553 or 746 bp enhancer fragments. Northern analysis of the rat enhancer fragments (553 and 746 bp) in pΦGH constructs transiently transfected into control and treated (LPS, TNF-α and IL-1β) rat pulmonary epithelial cells.

However, when these smaller DNA fragments were utilized, the previously observed stimulus-specific pattern of protein–DNA interactions with the larger enhancer fragments was lost (R. J. Rogers, unpublished work). Unlike our results with the larger fragments (Figure 3, bottom left and right panels), EMSA with the smaller fragments (50 bp and 30 bp) showed only constitutive binding patterns. We believe that protein–protein interactions are most likely a prerequisite for the stimulus-specific DNA binding, thus explaining the loss of stimulus-specific protein–DNA interaction in the smaller deletions of this complex regulatory element.

The inducible enhancer elements within rat and human *MnSOD* can act with a heterologous promoter

To determine whether the *MnSOD* enhancer could function with a heterologous promoter, the enhancer fragment was cloned in both orientations into the TKGH expression vector. The herpesvirus thymidine kinase (TK) promoter in this vector is a 200 bp minimal, TATA-containing promoter, quite dissimilar to the GC-rich, TATA- and CAAT-less *MnSOD* promoter. Results of transient transfections and Northern analysis (Figure 4, left panel) demonstrated that the enhancer element could co-operate with the minimal TK promoter and dramatically increase the transcriptional activity of the *hGH* reporter gene in response to LPS, TNF-α, and IL-1β. The element functioned equally well in both orientations and, interestingly, was able to orchestrate reporter induction to as much as 45-fold above baseline. The ability of this element to enhance transcriptional activity of both the endogenous and a heterologous promoter in an orientation-independent and position-independent manner further qualifies it as an enhancer element.

Given the potency of this enhancer element, we compared the sequence of intron 2 in the rat gene with the corresponding region in the human *MnSOD* locus and found a high level of homology. In order to evaluate the functional significance of this region, a 553 bp fragment of the rat enhancer and an analogous 466 bp region of intron 2 of human *MnSOD* were inserted into *Nde*I site of the TKGH vector. The ability of the fragments to cause inducible enhancer activity was assessed by transient transfections and Northern analysis. Both the rat and the human fragments caused essentially identical inducible expression in response to LPS, TNF-α and IL-1β (Figure 4, right panel), indicating that this region of human intron 2 likely acts as an enhancer in the endogenous gene and that the enhancer activity itself is well conserved between species. We have also demonstrated that the rat and human enhancer can function equally as well in human cell lines (R. J. Rogers, unpublished work).

Evaluation of promoter–enhancer interactions

We have demonstrated by *in vivo* footprinting that the *MnSOD* promoter contains ten potential basal protein-binding sites [18]. These sites are illustrated in Figure 5, top panel, relative to the restriction sites that were employed for the promoter-deletion analysis (Figure 1, top panel). To define the areas within the promoter required for interaction with the enhancer element, the previous promoter-deletion constructs [18] were coupled with a 919 bp enhancer fragment (Figure 5, top panel). Transient transfection and Northern analysis were used to evaluate inducible activity for these vector constructs. Of interest, the first five binding sites could be deleted without any detectable decrease in inducible activity (Figure 5, bottom left and right panels). It was not until the remaining five basal binding sites were eliminated that the level of induction decreased (Figure 5, bottom right panel) with almost complete loss of basal activity. Interestingly, LPS-inducible transcription could still occur when all previously defined promoter-protein-binding sites were deleted, but only when the vector construct contained the enhancer fragment (Figure 5, bottom right panel). However, in the absence of the enhancer element, deletion of the same promoter region, (construct Nae/E; see Figures 1, bottom left and right panels), eliminated any transcription, thus indicating that the enhancer element contained DNA sequence capable of independently promoting transcription in a stimulus-regulated manner.

The rat and human enhancer elements contain inducible promoter activity

With the results of the previous experiment (Figure 5, bottom right panel) we postulated that the enhancer element might exhibit stimulus-dependent promoter activity in the absence of a

true promoter. Since the Nae/E GH construct did contain 77 bp from the 5′ flanking region of the *MnSOD* promoter, the rat and the human enhancer elements were inserted into the promoter-less *hGH* vector (PΦGH) (Figure 6, left panel). Figure 6, left panel, shows the results of the 466 bp human enhancer fragment in the presence and absence of the TK promoter. Inducible transcription was observed with LPS, TNF-α and IL-1β, but at lower levels than when the fragment was inserted into the TKGH vector. Interestingly, two transcripts, one the correct size and one approx. 200–300 bp larger, were seen when the enhancer fragment acted as its own promoter. When the 553 bp and 746 bp rat enhancer fragments were tested in the promoter-less *hGH* vector (pΦGH), similar results to those obtained with the human fragment were obtained, in that two different-sized transcripts were observed (Figure 6). It was noteworthy, however, that when either the 553 bp or the 746 bp enhancer fragment was inserted into pΦGH in the 3′ to 5′ orientation, the correct-sized transcript predominated. This result would indicate that the enhancer can indeed act as a promoter, but its orientation and position relative to the start of transcription are important. To determine if the preceding hypothesis is correct, pΦGH vector constructs containing the 260 bp enhancer fragment were created. As can be seen in Figure 6, right panel, when the 260 bp enhancer fragment acting as a promoter was inserted into the pΦGH vector in the 3′-to-5′ orientation, a single stimulus-responsive transcript resulted.

DISCUSSION

As a cellular antioxidant, mitochondrial MnSOD has been consistently shown to be an effective cytoprotective enzyme. Expression of the *MnSOD* gene is highly regulated in response to a variety of pro-inflammatory mediators in many cell types. In rat lung epithelial cells, the inflammatory mediators LPS, TNF-α and IL-1β each cause MnSOD steady-state mRNA levels to increase 10–20-fold, which has been shown in nuclear run-on studies [17a] to be partly due to increased transcription of the gene. A survey of the entire *MnSOD* locus for sites of possible protein–DNA interaction using DNase-I-hypersensitive-site analysis revealed increased nuclease accessibility at sites in the 5′ proximal promoter region and six other sites located within the gene [18]. The present experiments further expand our understanding of the molecular mechanisms regulating basal and induced expression of *MnSOD* by identifying an enhancer region within the rat and human *MnSOD*.

The 5′ flanking sequence of *MnSOD* is characterized by a GC-rich island lacking a TATA- and CAAT-box for initiation of transcription. *In vivo* footprinting studies have defined protein-binding sites for ten basal transcription factors within 500 bp of the transcriptional start site [18]. Promoter-deletion analysis identified essential *cis*-acting sequences located within 157 bp of the transcriptional start site [18]. This region of the promoter includes five of the basal protein-binding sites and is capable of supporting basal and stimulated (LPS, TNF-α and IL-1β) expression. However, protein and mRNA levels of the *hGH* reporter were only induced 2–3-fold in transient transfection studies using vectors containing from 4.5 to 0.16 kb of the *MnSOD* promoter region alone [18]. Examination of the *MnSOD* promoter for known transcription-factor consensus sequences by computer analysis revealed an NF-κB sequence at -353 as well as Sp1 and gut-enriched Krüppel-like-factor (GKLF) [30,31] sites corresponding to binding sites I–V. As previously shown, the NF-κB site is not, on the basis of *in vivo* footprinting data, occupied, and it is not important for enhancer function (Figure 5 , bottom left panel). On the other hand, guanine contacts from *in vitro* footprinting with purified Sp1 and GKLF strongly implicates these proteins with the *in vivo* contacts observed at sites I–V. However, previous data [18] and Figure 5, bottom right panel, seem to indicate that, on the basis of transient transfection studies, the potential Sp1 and GKLF sites (I–V) are not essential for basal or enhancer-dependent gene expression (using LPS, TNF-α, and IL-1β as stimulants). These data may be reconciled by appreciating that constitutive Sp1 and/or GKLF binding to sites I–V might be necessary for other stimuli known to induce (INF-γ [32,33], phorbol ester [34]) or inhibit (glucocorticoids [35]) *MnSOD* expression. Alternatively, it should be noted that the functional data were obtained by transient transfection of plasmid reporter gene DNA into mammalian cells; consequently it is possible that the plasmid DNA does not form proper chromatin structures following transfection. Appropriate chromatin structure is very likely crucial for the correct alignment of the DNA sequence important for the promoter–enhancer interactions. Therefore we must consider this as a possible explanation for the results shown in Figure 5, bottom right panel. The data in Figure 5, bottom right panel, do, however, strongly implicate the functional importance of binding sites VI–X to both basal and enhancer/stimulus-specific expression. The pNae/Eag GH vector was not sufficient to drive either basal or stimulated expression [18], suggesting that a minimal promoter sequence for transcriptional initiation was no longer present.

The observed induction of the reporter gene from the 5′ *MnSOD* promoter was much lower than endogenous *MnSOD* expression following treatment with inflammatory mediators [18]. These data and the presence of DNase-I-hypersensitive sites within the gene suggested that regulatory elements might exist outside the 5′ flanking sequence. Results from transfections with vectors combining both the 5′ promoter region and the internal 6.1 kb fragment (containing the remainder of the DNase-I-hypersensitive sites) confirmed that genomic sequences 3′ to the transcriptional start site contain enhancer activity. Most importantly, this region contains adequate enhancer activity to mimic endogenous, stimulus-dependent transcription levels. Deletion analysis of this region localized this activity to a 260 bp area within intron 2, which contains DNase-I-hypersensitive site 2. When this 260 bp region is divided into two 143 bp fragments, we found that each of these fragments independently retained inducible activity, albeit at a lower level. Moreover, on the basis of EMSA, these same 143 bp fragments were able to bind both constitutive nuclear factors as well as a number of factors specific to extracts from induced cells. However, attempts to further delineate the enhancer by EMSA using DNA fragments less than 50 bp (R. J. Rogers, unpublished work) led to the elimination of stimulus-specific *in vitro* binding, further demonstrating the complexity of this enhancer and implying that protein–protein interactions may be critical to the formation of specific protein–DNA complexes between the promoter and enhancer. Therefore we believe that this enhancer is composed of a set of complex interacting elements involved in the inducible expression of *MnSOD*. Contrary to the published characterization of the murine gene [36], our data would indicate that separate elements within this enhancer region retain an ability to induce *MnSOD* transcriptional activity, but that small (25–30 bp) individual elements cannot act independently to confer the inducible levels seen in the endogenous gene.

Our results demonstrate that this enhancer element requires a portion of the *MnSOD* promoter to achieve levels of induction analogous to steady-state Northern analysis. Using portions of the promoter coupled with the enhancer, we demonstrated the requirement for sequences from -154 to the start of transcription, which include protein-binding sites VI–X defined by *in*

vivo footprinting by Kuo et al. [18]. Given the functional connection between the enhancer and the *MnSOD* promoter, we postulate that the enhancer may interact with the promoter through a mechanism involving DNA bending [37]. As support for this hypothesis, we have performed co-transfection experiments with the promoter and enhancer on separate plasmids and found under these conditions that inducible transcription could not be achieved (R. J. Rogers, unpublished work). This substantiates the argument that the *MnSOD* promoter and enhancer must reside within a contiguous region of DNA. Therefore regulatory elements most likely physically interact through DNA bending, as proposed by Ptashne [37], and possibly involving an alteration in chromatin structure in the promoter as defined by Kuo et al. [18].

Of particular interest is the existence of a homologous functional enhancer element in human *MnSOD* (Figure 4, right panel) that responds to the same inflammatory mediators as the rat enhancer in both rat and human cells (results not shown). In addition, another unique characteristic of the rat and human enhancer element is its ability to drive transcription independent of a classical promoter (Figure 6). As an independent promoter/regulatory element, this sequence has the capacity to promote stimulus-dependent transcription with negligible basal levels. Previous work in our laboratory explored the possibility of an alternative promoter or differential mRNA splicing as a cause for the multiple transcripts in the rat. Using primer extension and ^{32}P-labelled cDNA and genomic fragments as hybridization probes, it was determined that alternative polyadenylation was the likely cause for the multiple transcripts seen in the rat *MnSOD* [24]. Understanding the regulation of this enhancer region will be important, since it seems to be exquisitely responsive to acute cytokine mediators and, if similar motifs are found in other genes, may exist as a regulatory unit that serves as a general inflammatory response element. Current efforts are underway to further characterize the enhancer by DMS *in vivo* footprinting and mutagenesis for functional transfection studies.

The technical assistance of Gail Rampersaud in portions of this project is greatly appreciated. This work was supported by National Institutes of Health grant RO1 HL39593 to H. N.

REFERENCES

1 Halliwell, B. and Gutteridge, J. M. (1990) Methods Enzymol. **186**, 1–85
2 Visner, G. A., Block, E. R., Burr, I. M. and Nick, H. S. (1991) Am. J. Physiol. Lung Cell. Mol. Physiol. **260**, L444–L449
3 Dougall, W. C. and Nick, H. S. (1991) Endocrinology (Baltimore) **129**, 2376–2384
4 Suzuki, K., Tatsumi, H., Satoh, S., Senda, T., Nakata, T., Fujii, J. and Taniguchi, N. (1993) Am. J. Physiol. **265**, H1173–H1178
5 Del Maestro, R. and McDonald, W. (1989) Mech. Aging Dev. **48**(1), 15–31
6 Shull, S., Heintz, N. H., Periasamy, M., Manohar, M., Janssen, Y. M., Marsh, J. P. and Mossman, B. T. (1991) J. Biol. Chem. **266**, 24398–24403
7 Wong, G. H. and Goeddel, D. V. (1988) Science **242**, 941–944
8 Wong, G. H., Elwell, J., Oberly, L. and Goeddel, D. V. (1989) Cell **58**, 923–931
9 Visner, G. A., Dougall, W. C., Wilson, J. M., Burr, I. M. and Nick, H. S. (1990) J. Biol. Chem. **265**, 2856–2864
10 Eastgate, J., Moreb, J., Nick, H. S., Suzuki, K., Taniguchi, N. and Zucali, J. R. (1993) Blood **81**, 639–646
11 Akashi, M., Hachiya, M., Paquette, R. L., Osawa, Y., Shimizu, S. and Suzuki, G. (1995) J. Biol. Chem. **270**, 15864–15869
12 Manganaro, F., Chopra, V. S., Mydlarski, M. B., Bernatchez, G. and Schipper, H. M. (1995) Free Radicals Biol. Med. **19**(6), 823–835
13 Baker, K., Marcus, C. B., Huffman, K., Kruk, H., Malfroy, B. and Doctrow, S. R. (1998) J. Pharmacol. Exp. Ther. **284**(1), 215–221
14 Wispe, J. R., Warner, B. B., Clark, J. C., Dey, C. R., Neuman, J., Glasser, S. W., Crapo, J. D., Chang, L. and Whitsett, J. A. (1992) J. Biol. Chem. **267**, 23937–23941
15 Li, Y., Huang, T.-T., Carlson, E. J., Melov, S., Ursell, P. C., Olson, J. L., Noble, L. J., Yoshimura, M. P., Berger, C., Chan, P. H. et al. (1995) Nat. Genet. **11**, 376–381
16 Melov, S., Schneider, J. A., Day, B. J., Hinerfeld, D., Coskun, P., Mirra, S. S., Crapo, J. D. and Wallace, D. C. (1998) Nat. Genet. **18**, 159–163
17 Visner, G. A., Chesrown, S. E., Monnier, J., Ryan, U. and Nick, H. S. (1992) Biochem. Biophys. Res. Commun. **188**, 453–462
17a Hsu, J.-L. (1993) Thesis Dissertation, pp. 49–52, University of Florida, Gainsville
18 Kuo, S., Chesrown, S. E., Mellot, J., Rogers, R. J., Hsu, J.-L. and Nick, H. S. (1999) J. Biol. Chem. **274**, 3345–3354
19 Queen, C. and Baltimore, D. (1983) Cell **33**, 741–748
20 Judde, J. and Max, E. E. (1992) Mol. Cell. Biol. **12**, 5206–5216
21 Takimoto, Y. and Kuramoto, A. (1993) Jpn. J. Cancer Res. **84**, 1268–1272
22 Callis, J., Fromm, M. and Walbot, V. (1987) Genes Dev. **1**, 1183–1200
23 Simkevich, C. P., Thompson, J. P., Poppleton, H. and Raghow, R. (1992) Biochem. J. **286**, 179–185
24 Hurt, J., Hsu, J.-L., Dougall, W. C., Visner, G. A., Burr, I. M. and Nick, H. S. (1992) Nucleic Acids Res. **20**, 2985–2990
25 Kriegler, M. (1990) Gene Transfer and Expression: A Laboratory Manual, pp. 96–100, Stockton Press, New York
26 Chomczynski, P. and Sacchi, N. (1987) Anal. Biochem. **162**, 156–159
27 Selden, R. F., Howie, K. B., Rowe, M. E., Goodman, H. M. and Moore, D. D. (1986) Mol. Cell. Biol. **6**, 3173–3179
28 Fried, M. G. and Crothers, D. M. (1981) Nucleic Acids Res. **9**, 6505–6525
29 Andrews, N. C. and Faller, D. V. (1991) Nucleic Acids Res. **19**, 2499
30 Shields, J. M. and Yang, V. W. (1998) Nucleic Acids Res. **26**, 796–802
31 Zhang, W., Shields, J. M., Sogawa, K., Fujii-Kuriyama, Y. and Yang, V. W. (1998) J. Biol. Chem. **273**, 17917–17925
32 Harris, C. A., Derbin, K. S., Hunte McDonough, B., Krauss, M. R., Chen, K. T., Smith, D. M. and Epstein, L. B. (1991) J. Immunol. **147**, 149–154
33 Valentine, J. F. and Nick, H. S. (1992) Gastroenterology **103**, 905–912
34 Fujii, J. and Taniguchi, N. (1991) J. Biol. Chem. **266**, 23142–23146
35 Dougall, W. C. and Nick, H. S. (1991) Endocrinology (Baltimore) **129**, 2376–2384
36 Jones, P. L., Dongsheng, P. and Boss, J. M. (1997) Mol. Cell. Biol. **17**, 6970–6981
37 Ptashne, M. (1986) Nature (London) **322**, 697–701

Received 23 August 1999/4 January 2000; accepted 27 January 2000